Electronic Supplementary Information

Plant-to-planet analysis of CO_2-based methanol processes

Andres Gonzalez-Garay,[a] Matthias S. Frei,[b] Amjad Al-Qahtani,[a] Cecilia Mondelli,[b,*] Gonzalo Guillén-Gosálbez,[b,*] and Javier Pérez-Ramírez[b,*]

[a] Centre for Process Systems Engineering, Imperial College London, SW7 2AZ London, United Kingdom.

[b] Institute for Chemical and Bioengineering, Department of Chemistry and Applied Biosciences, ETH Zurich, Vladimir-Prelog-Weg 1, 8093 Zurich, Switzerland.
E-mail addresses: cecilia.mondelli@chem.ethz.ch; gonzalo.guillen.gosalbez@chem.eth.ch; jpr@chem.ethz.ch

This document is structured in six parts. Section 1 provides details on the process modelling of the fossil- and CO_2-based methanol synthesis routes. In Section 2, additional information on the life-cycle analysis (LCA) is given, namely, the data sources employed in the life-cycle inventory (LCI) calculations, a discussion on the scope definition, the monetary values used to monetise environmental and health impacts, and the assumptions made. In Section 3, the results of the various process optimisations are displayed, including the optimal operating conditions, process yields and conversion and selectivity per pass. Section 4 provides the full LCA results at the endpoint and disaggregated midpoint levels, including their breakdown into reactants, utilities and steel. Section 5 provides the methodology followed in the estimation of future hydrogen prices. Finally, Section 6 presents the results obtained through the application of planetary boundaries (PBs) when considering CO_2 captured from natural gas (NG) power plants and directly from air (DAC) and outlines the current limitations of this method.

1. Process modelling of methanol production

In essence, both the process based on fossil-derived syngas and the one based on CO_2 and renewable hydrogen lead to very similar flowsheets, mainly comprising a reactor unit followed by two flash separators and a distillation column implementing different operating conditions depending on the specific case.

The traditional syngas-based process was modelled according to Luyben.[1] Here, a stream containing 11,450 kmol h^{-1} of syngas at 50°C and 51 bar is compressed to 75 bar, cooled to 38°C, and pressurised again to 110 bar, which corresponds to the operating pressure in the reactor. The syngas, generated by steam reforming of natural gas (NG), has a mole composition of 67.47% H_2, 22.97% CO, 6.86% CO_2, 0.23% H_2O, 2.17% CH_4, and 0.3% N_2. The pressurised stream of syngas is mixed with three recycled streams, and then heated to 150°C before being fed to the reactor. The latter is a plug-flow reactor (PFR) holding a packed catalyst bed with a volume of 100 m^3. The Cu-ZnO-Al_2O_3 catalyst follows the kinetics already reported by Vanden Bussche and Froment.[2] The heat released upon reaction is used to generate high-pressure steam at 254°C and 42 bar. The effluent of the reactor exiting the unit at 266°C is cooled down to 38°C, and then sent to the first flash separator. Part of the gas stream in this unit is pressurised to 110 bar and recycled back to the process, while the rest is released to the environment through a purge, which contains 49.7% H_2, 32.6% CH_4, 8.6% CO_2, 4.5% N_2, 4.1% CO, and 0.5% methanol. The liquid stream is depressurised to 2 bar and fed into a second flash separator. The gas stream from the second flash is again pressurised to 110 bar and recycled to the process, while the liquid stream is sent to a distillation column. The column implements a partial condenser, where the gases collected are pressurised and recycled back to the process. The liquid stream retrieved from the condenser contains methanol with a molar purity of 99.9%, while the liquid stream at the bottom of the column mostly comprises water, which is recovered and sent to a wastewater treatment unit.

In the CO_2-based process, CO_2 is available at 25°C and 1 bar. Hence, its pressure is firstly increased to match the reactor conditions, *i.e.*, 50 bar. Hydrogen is available at 30 bar and needs to be compressed to reach the same pressure. The two gases are mixed with a recycled stream and heated between 180-280°C to carry out the reaction at 50 bar.[2] As in the previous case, the outlet stream is cooled down and sent to a flash unit, where part of the vapour stream containing CO_2, hydrogen and CO is recovered and recycled back to the reactor, while a certain amount is purged to avoid the build-up of species within the system. This purge contains unreacted H_2 (≈80%), CO_2 (≈10%), CO (≈4%), methanol (≈6%), and water (<1%). The liquid stream leaving the flash unit is depressurised to 2 bar, and then sent to a second flash unit, where most of the remaining gases are separated from water and methanol. The liquid stream from the second flash separator is heated to 80°C and then fed to a distillation column, where methanol is recovered with a molar purity of 99.9 %. The gaseous emissions from the first flash unit are used to generate steam at high pressure in a furnace added to the conventional flowsheet. Two different reactor models were implemented in the CO_2-based flowsheet. The first was an equilibrium reactor providing the best possible performance based on the thermodynamic limit of the reaction system. In essence, this model implements an ideal catalyst attaining the equilibrium in the main reaction, *i.e.*, CO_2 hydrogenation, while fully inhibiting the unwanted parallel reverse water-gas shift (RWGS) reaction. The second was a plug-flow reactor loaded with the Cu-ZnO-Al_2O_3 catalyst following the same kinetic model previously mentioned.[2] In both cases, the fresh CO_2 feed was fixed to 2,000 kmol h^{-1} to ensure a minimum annual production of 440 kton y^{-1}, a value often found for conventional plants.[3]

Hence, overall, three rigorous models were developed in Aspen-HYSYS v9: (i) the business-as-usual process producing methanol from syngas from natural gas, the operating conditions of which were not optimised in this work but rather fixed to the values reported by Luyben;[1] (ii) CO_2 hydrogenation over an ideal catalyst reaching the thermodynamic limit; and (iii) the same CO_2-based process implementing the copper-based catalyst. The optimisation of the two CO_2-based flowsheets was performed using a genetic algorithm coupled with the simulation model in Aspen-HYSYS, where the decision variables optimised correspond to temperature and pressure in the reactor, and hydrogen fresh feed and purge ratio for the ideal flowsheet, and volume and temperature of the reactor, and hydrogen fresh feed and purge ratio for the one based on the Cu-ZnO-Al_2O_3 catalyst. Given that equilibrium reactors produce the same results regardless of the reactor volume, *i.e.*, equilibrium is assumed to be attained instantly, the volume was set at a standard value of 63 m^3 in the ideal CO_2-based scenario.[4] An additional compressor was included when the hydrogen feed pressure in the optimisation raised above 30 bar (hydrogen feed pressure). In the copper catalyst-based process, the pressure was fixed to 50 bar, as reported in the original source of the kinetic data for the Cu-ZnO-Al_2O_3 catalyst.[2] The ordinary differential equations system that models the kinetics was solved with Aspen-HYSYS by defining the corresponding kinetic expression in the reactor model. During the optimisation of the flowsheets, heat integration was performed using the targets obtained with the composite curve. Once the optimum value was found, a detailed heat exchanger network design was carried out applying the MINLP approach of Yee and Grossmann.[5]

The OPEX of the various flowsheets were estimated using the cost parameters listed in **Table S1**, while the CAPEX were calculated using the correlations and standard economic parameters given by Sinnot and Towler,[6] considering the installation factors reported therein for each equipment unit, and estimating the annualised capital cost with Equation 9.26 in the original source.[6] All the cost values were expressed in 2015USD. CAPEX from year 2010 where projected to year 2015 using the CEPCI index, with a value of 570.5.

Table S1. Cost parameters used in the OPEX calculations.

Flow	Cost (USD $unit^{-1}$)
CO_2 coal-based power plant[7] (kg)	0.047
CO_2 natural gas-based power plant[7] (kg)	0.075
CO_2 direct air capture[8] (kg)	0.16
H_2 biomass[9] (kg)	2.24
H_2 nuclear[9] (kg)	4.63
H_2 wind[9] (kg)	5.24
H_2 solar[9] (kg)	8.87
Steam[10] (ton)	14.30
Electricity[3] (MWh)	104.61
Cooling water[3] (m^3)	$3.30 \cdot 10^{-2}$
Catalyst (kg)	125.00
Heat recovery[11] (ton of steam)	7.70
Wastewater to be treated[4] (m^3)	1.50
Hydrogen from water electrolysis in 2030	**Cost (USD $unit^{-1}$)**
AEC electrolyser + nuclear electricity (kg)	2.27-3.92
PEMEC electrolyser + wind electricity (kg)	2.03-5.39
SOEC electrolyser + solar electricity (kg)	2.12-7.26
AEC electrolyser + nuclear electricity (kg)	2.25-3.78
PEMEC electrolyser + wind electricity (kg)	2.06-5.26
SOEC electrolyser + solar electricity (kg)	2.15-7.16
AEC electrolyser + nuclear electricity (kg)	2.39-3.70
PEMEC electrolyser + wind electricity (kg)	2.18-5.17
SOEC electrolyser + solar electricity (kg)	2.26-7.10

AEC: alkaline electrolysis cell, PEMEC: proton-exchange membrane electrolysis cell, SOEC: solid oxide electrolysis cell.

2. LCA of methanol production and its limitations

The LCA results for the BAU process were directly taken from the Ecoinvent database version 3.4,[12] while a full LCA encompassing the four LCA phases was applied to assess the methanol production process from CO_2 and hydrogen procured from various sources, using Recipe 2016 to quantify the environmental impacts on human health, ecosystem quality and resource scarcity. The units for the endpoints are as follows.[13] DALYs (disability adjusted life years), used to quantify human health, represent the years that are lost or during which a person is disabled due to a disease or accident. Ecosystem quality is measured in local species loss integrated over time (species year). Finally, resource scarcity, quantified in US-dollars, represents the extra costs involved for future mineral and fossil resource extraction.

Concerning the scope of the analysis, we note that recent studies expanded the system boundaries in the assessment of green methanol to evaluate the alternative use of the same amount of renewable energy and carbon captured required for its production in the decarbonisation of the electricity mix of a country, ultimately questioning its mitigation potential.[14] Notwithstanding the role of system boundaries in our assessment, a cradle-to-gate scope was adopted that covers direct emissions and waste at the plant level together with those burdens embodied in the methanol process inputs, *i.e.*, H_2, CO_2, electricity, heat and steel. Hence, the end-use phase and any alternative use of renewable energy and carbon capture were omitted in our analysis. The motivation for this was twofold. Firstly, the use phase of methanol, either as platform chemical or fuel, is the same across technologies and, therefore, its inclusion would add no discriminatory power to the analysis. Secondly, evaluating alternative uses of renewable energy and carbon capture and storage, *i.e.*, methanol production *vs.* decarbonisation of the electricity mix, would require the detailed consideration of capacity and reliability constraints of a specific national mix, which is out of the scope of this work.

The LCI entries for methanol production were obtained from the mass and energy flows embodied in its inputs, *i.e.*, H_2, CO_2, electricity, heat and steel, plus the direct emissions and waste generated in the main process flowsheet. The inventory flows embodied in H_2 and CO_2 are given in **Tables S2** and **S3**, respectively. The LCI entries embodied in electricity, heat and steel were retrieved from Ecoinvent v3.4, as described in **Table S4**, which also displays the inventory flows used in the quantification of the impact embodied in hydrogen and CO_2. Finally, **Table S5** shows the inputs and outputs for each flowsheet, namely, the amount of H_2, CO_2, electricity, heat and steel consumed as well as the direct emissions and waste of the main methanol process for each hydrogen source and considering that the CO_2 is captured from coal plants.

A monetisation method was then applied to express LCA impacts on a common monetary basis that enables a more straightforward comparison of scenarios. The approach reported by Weidema[15] was followed, in which the endpoint categories of human health, ecosystem quality and resource scarcity in the ReCiPe LCIA method are monetised using specific economic penalties. The monetary factors applied were $7.4 \cdot 10^3$ EUR2003 per 1 DALY in the human health category and $9.5 \cdot 10^6$ EUR2003 per 1 lost species in the ecosystem quality indicator. The resources depletion indicator is already expressed in monetary values (USD2003). ReCiPe 2016 was applied in all of the LCA calculations, updating the monetary factors of the human health and ecosystems category to USD2015 by applying a factor of 1.41. The category of resources depletion was updated to USD2015 using a factor of 1.25.

The main limitations of the LCA study are summarised hereon:

- Consistent with the literature,[16] the impact embodied in the electrolyser was considered as negligible compared to the total impact of hydrogen production *via* water electrolysis. This is because the impact embodied in the electricity powering the electrolyser has been shown to be the main contributor to the total hydrogen impact.
- Similarly, following the literature sources used to model the CO_2 capture technologies,[8,17,18] the impact embodied in the CO_2 capture facilities was neglected. The reason for this is, again, that the impact embodied in the amount of energy required to desorb the CO_2 from the absorbent is the main contributor to the total impact.
- Fugitive emissions from equipment units were neglected, while the impact embodied in the catalyst was also omitted. This is a common practice in many LCA studies of chemical processes, where the main contributors to the total impact are raw materials and energy consumption.[19]

- We consider that the impact of the construction phase can be approximated by the impact embodied in the equivalent amount of stainless steel contained in the equipment units. This impact of construction is often either neglected or approximated with the same simplification we adopt here.[6]
- Additional assumptions and simplifications are explained in the description of the background data retrieved from Ecoinvent 3.4, which is summarised in Table S4.

Table S2. Inventory flows of the foreground system per kilogram of hydrogen at 30 bar.

Technology	Biomass[20] gasification for oil poplar-wood chips	Nuclear-powered[21] water electrolysis	Solar-powered[22] water electrolysis	Wind-powered[23] water electrolysis
By-products	0.85 kg hard coal	n.a.	n.a.	n.a.
Materials (inputs)				
Tap water (kg)	20.59	18.04	18.04	18.04
Electricity (kWh)	3.76	52.26	52.26	52.26
Wood chips	18.15	-	-	-
Natural gas (m^3)	$1.88 \cdot 10^{-3}$	-	-	-
Transport (tkm)	1.19	-	-	-
Waste (undesired outputs)				
Waste wood, sanitary landfill (kg)	$1.81 \cdot 10^{-4}$	-	-	-
Wastewater treatment plant residuals, to unsanitary landfill (kg)	10.97	-	-	-
Direct emissions (undesired outputs)				
CO_2 (kg)	21.43	-	-	-
SO_2 (kg)	$2.69 \cdot 10^{-3}$	-	-	-
NO_2 (kg)	$4.03 \cdot 10^{-3}$	-	-	-
HCl (kg)	$6.98 \cdot 10^{-4}$	-	-	-
Particulates, unspecified (kg)	$1.97 \cdot 10^{-4}$	-	-	-

Table S3. Inventory flows of the foreground system per kilogram of CO_2 captured at 1 bar.

Technology	Capture from coal power plant using chemical absorption with monoethanolamine[17]	Capture from natural gas power plant using chemical absorption with monoethanolamine[18]	Capture from direct air capture using an aqueous KOH sorbent coupled to a calcium caustic recovery loop[8]
By-products	Electricity: 0.775 kWh	Electricity: 3.23 kWh	-
Materials (inputs)			
Air (kg)	-	20.19	-
Water (kg)	-	1.5161	3.105
Natural gas (m^3)	0.00078	0.8636	0.1895
Catalyst (mg)	-	2.97	-
Electricity (kWh)	-	-	0.366
Calcium carbonate (kg)	-	-	0.02
Limestone (kg)	0.04263	-	-
Light fuel oil (kg)	0.00620	-	-
Hard coal (kg)	0.52093	-	-
Monoethanolamine (kg)	0.00155	0.0088	-
NaOH (kg)	0.00012	-	-
NH_3 (kg)	0.00115	-	-
Waste (undesired outputs)			
Municipal solid waste, to sanitary landfill	0.00406	-	-
Wastewater (kg)	-	1.6452	-
Catalyst disposal (mg)	-	2.97	-
Direct emissions to air (undesired outputs)			
CO_2 (kg)	0.05240	0.3286	-
SO_2 (kg)	0.00007	-	-
NO (kg)	0.00106	0.0016	-
Particulates, unspecified (kg)	0.00011	-	-
NH_3 (kg)	0.00027	-	-
Monoethanolamine (kg)	0.00009	0.0035	-

Table S4. Inventory flows of the foreground system retrieved from Ecoinvent v3.4.

Flow	Technology involved	Description in Ecoinvent
NH_3	CO_2 coal	Ammonia at plant as 100% NH_3
Electricity from nuclear consumed by water electrolysis	H_2 nuclear	Electricity, high voltage electricity production, nuclear, pressure water reactor
Electricity from solar consumed by water electrolysis	H_2 solar	Electricity production, photovoltaic, 570 kWp open ground installation, multi-Si
Electricity from wind consumed by water electrolysis	H_2 wind	Electricity, high voltage electricity production, wind, <1MW turbine, onshore (86.1%); electricity, high voltage [RoW] electricity production, wind, 1-3MW turbine, offshore (13.9%)
Electricity high voltage	All	Electricity, high voltage, production mix
Hard coal	CO_2 coal	Market for hard coal
Heat	Methanol	Market for heat, from steam, in chemical industry
Light fuel oil	CO_2 coal	Light fuel oil, petroleum refinery operation
Limestone	CO_2 coal	Limestone from nature
Monoethanolamine	CO_2 coal and NG	Market for monoethanolamine
Municipal solid waste, to sanitary landfill	CO_2 coal	Disposal municipal solid waste, 22.9% water to sanitary landfill
Natural gas	Methanol / CO_2 NG and DAC	Natural gas production
NaOH	CO_2 coal	Production mix sodium hydroxide (50% NaOH)
Water	H_2 biomass / CO_2 NG and DAC	Market for tap water
Calcium carbonate	CO_2 DAC	Market for calcium carbonate, precipitated
Steel production	Methanol	Steel production, converter, chromium steel 18/8
Catalyst	CO_2 NG	Market for spent automobile catalyst
Tap water	H_2	Tap water production, conventional treatment
Transport	H_2 biomass	Transport: transport, freight, lorry 16-32 metric ton, EURO4
Waste wood sanitary landfills	H_2 biomass	Waste wood sanitary landfill: treatment of waste wood, untreated, sanitary landfill
Wastewater treatment plant residuals, to unsanitary landfill	H_2 biomass	Wastewater treatment plant residuals, to unsanitary landfill: treatment of residue from cooling tower, sanitary landfill
Wastewater	CO_2 NG	Market for wastewater, average
Catalyst disposal	CO_2 NG	Treatment of spent catalyst base from ethyleneoxide production, residual material landfill
Wood chips	H_2 biomass	Wood chips, wet, measured as dry mass

Table S5. Inputs/outputs of the main flowsheet per kilogram of methanol produced.

Inputs/outputs	H_2 biomass	H_2 nuclear	H_2 solar	H_2 wind
Raw materials				
CO_2 (kg)	1.50	1.47	1.45	1.45
Hydrogen (kg)	0.20	0.19	0.19	0.19
Utilities				
Cooling water (MJ)	4.96	4.97	4.97	4.95
Heating (MJ)	0	0	0	0
Electricity (kW)	0.30	0.30	0.30	0.30
Heat recovered (MJ)	0.44	0.48	0.42	0.39
Emission and waste				
CO_2 (kg)	0.110831	0.093737	0.075773	0.077025
Methanol (kg)	0.010091	0.010091	0.010091	0.010091
NO_2 (kg)	0.000181	0.000194	0.000170	0.000178
Wastewater, average (m^3)	$5.75\cdot10^{-4}$	$5.70\cdot10^{-4}$	$5.72\cdot10^{-4}$	$5.71\cdot10^{-4}$

3. Process modelling results

Table S6 summarises the optimal values of the decision variables for the various cases, where values in italics denote variables that were optimised while all others were fixed according to the original sources.[2,4]

Table S6. Optimisation results for the fossil- and CO_2-based methanol synthesis process scenarios. Decision variables optimised are shown in italics.

Model		Reactor V (m^3)	Reactor P (bar)	Reactor T (°C)	H_2 feed (kmol h^{-1})	Purge released (%)	Y_{MeOH} (%)	X_{COx} (%)	S_{MeOH} (%)
BAU		100	110	250	11,450 (syngas)	2.2	96.6	33.4	100
H_2 biomass	ideal	63	*29*	*108*	*5,872*	*0.22*	96.4	24.2	99.97
	Cu-ZnO-Al_2O_3	*50*	50	*221*	*5,894*	*0.25*	91.5	12.4	99.30
H_2 nuclear	ideal	63	*24*	*107*	*5,926*	*0.16*	97.2	24.6	99.98
	Cu-ZnO-Al_2O_3	*50*	50	*230*	*5,776*	*0.25*	93.4	13.6	99.8
H_2 solar	ideal	63	*31*	*131*	*5,828*	*0.11*	96.0	20.0	99.99
	Cu-ZnO-Al_2O_3	*50*	50	*228*	*5,842*	*0.21*	93.6	15.7	99.52
H_2 wind	ideal	63	*32*	*101*	*5,911*	*0.56*	98.5	35.0	99.97
	Cu-ZnO-Al_2O_3	*51*	50	*228*	*5,842*	*0.23*	93.8	15.8	99.55

Y_{MeOH} = overall process yield, *i.e.*, moles of methanol obtained as final product per mole of CO or CO_2 in the feed of the flowsheet.
X_{COx} = conversion of CO or CO_2 per pass, *i.e.*, moles of CO or CO_2 converted in the reactor per mole of CO or CO_2 fed to the reactor.
S_{MeOH} = methanol selectivity per pass, *i.e.*, moles of CO or CO_2 converted into methanol in the reactor per mole of CO or CO_2 reacted in the reactor.

4. LCA results

Figure S1 and **S2** depict the endpoint and disaggregated midpoint indicators for the BAU methanol process and the alternative processes based on CO_2 captured from coal power plants, from NG power plants and through DAC, and renewable hydrogen from distinct sources. It can be clearly seen how burden shifting takes place at both the midpoint and endpoint levels. Focusing on the case of CO_2 from coal at the endpoint level, this only occurs in methanol synthesis using biomass- and solar-based hydrogen. The process improves in relation to resources but worsens in terms of human health in both cases, and additionally worsens in terms of ecosystem quality with biomass-derived hydrogen. In contrast, methanol production employing wind- and nuclear-based hydrogen is superior to fossil-based methanol synthesis in all three impact categories. At the midpoint level, burden shifting takes place in several indicators, with the severity of this phenomenon depending on the specific impact category and hydrogen source.

Figure S3 provides the cost of methanol, including externalities, for all of the process scenarios considered. Note that, methanol from CO_2, regardless of its source, and biomass-based hydrogen performs significantly worse than fossil methanol due to the large impact embodied in hydrogen procurement. The biomass type considered in the analysis is wood chips in hardwood, for which Ecoinvent provides values of CO_2 captured from air (CO_2 fixation) of 0.477 $kg_{CO2\text{-}eq}\ kg_{biomass}^{-1}$. This value is way below to the 1.01 $kg_{CO2\text{-}eq}\ kg_{biomass}^{-1}$ reported in the original source[24], which includes not only the CO_2 fixation from air, but also the emissions coming from land transformation which are omitted in our analysis given the uncertainty associated with the quantification method. The amount of CO_2 captured by the biomass in our model cannot offset the emissions of the gasification process, ultimately leading to a carbon-positive methanol. This and other choices made in the last version of Ecoinvent, which was used for consistency across technologies, lead to discrepancies with the LCA values for biomass-based hydrogen reported in the original source, *i.e.*, 3.79 *vs.* 16.4 $kg_{CO2\text{-}eq}\ kg_{H2}^{-1}$. In any case, we found a large variability in the environmental impact of biomass, particularly in the CO_2 fixated per kg of biomass across biomass types in Ecoinvent, *e.g.*, 0.477-1.63 $kg_{CO2\text{-}eq}\ kg_{biomass}^{-1}$. The recommendation is, therefore, to take the LCA and PB results for the biomass-related scenario with caution, as they are highly dependent on the biomass source, which shows a strong regional dependency.

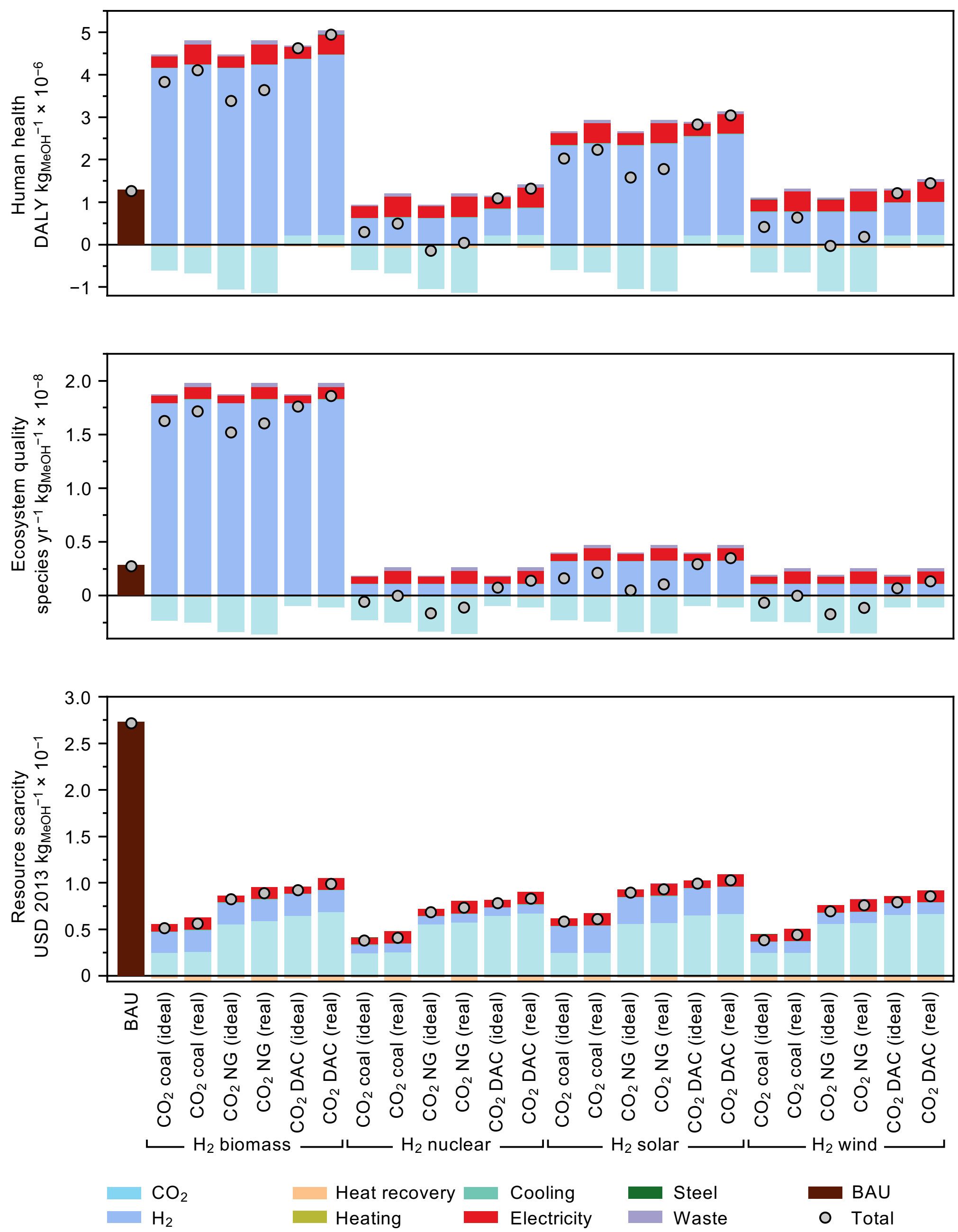

Figure S1. ReCiPe 2016 LCI analysis at the endpoint level of all methanol process scenarios analysed.

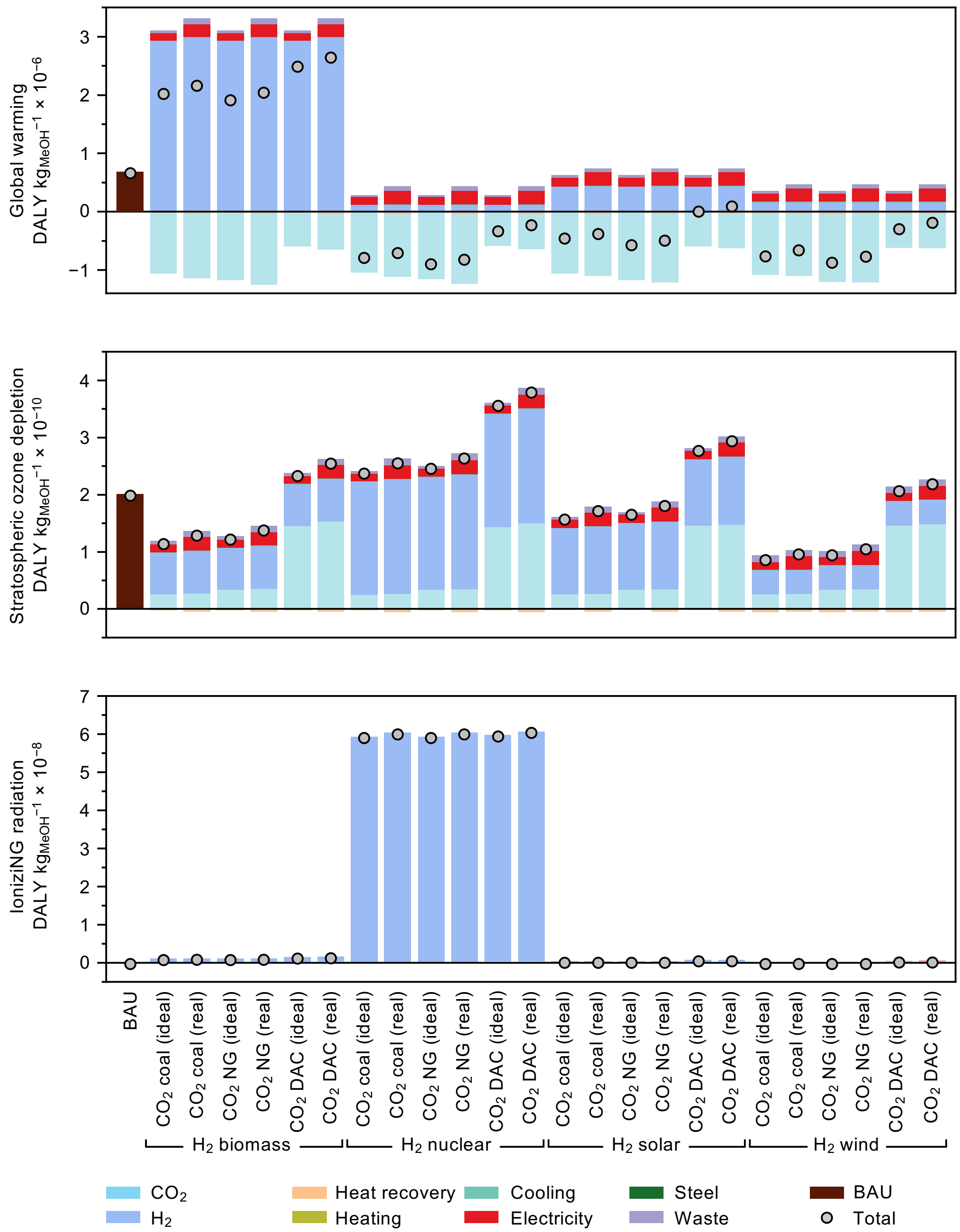

Figure S2a. ReCiPe 2016 LCI analysis at the midpoint level of all methanol process scenarios analysed, contributions to human health.

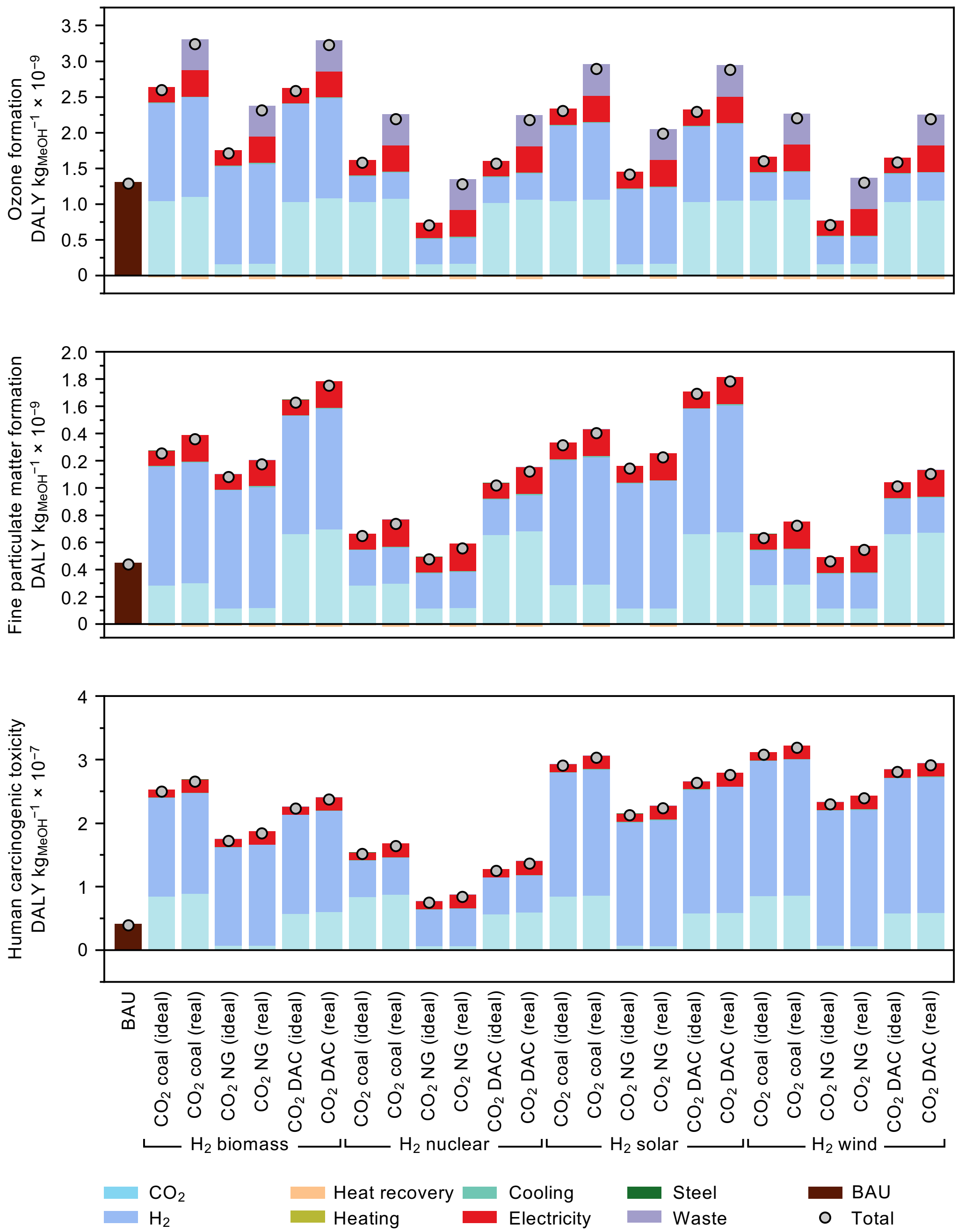

Figure S2a continued. ReCiPe 2016 LCI analysis at the midpoint level of all methanol process scenarios analysed, contributions to human health.

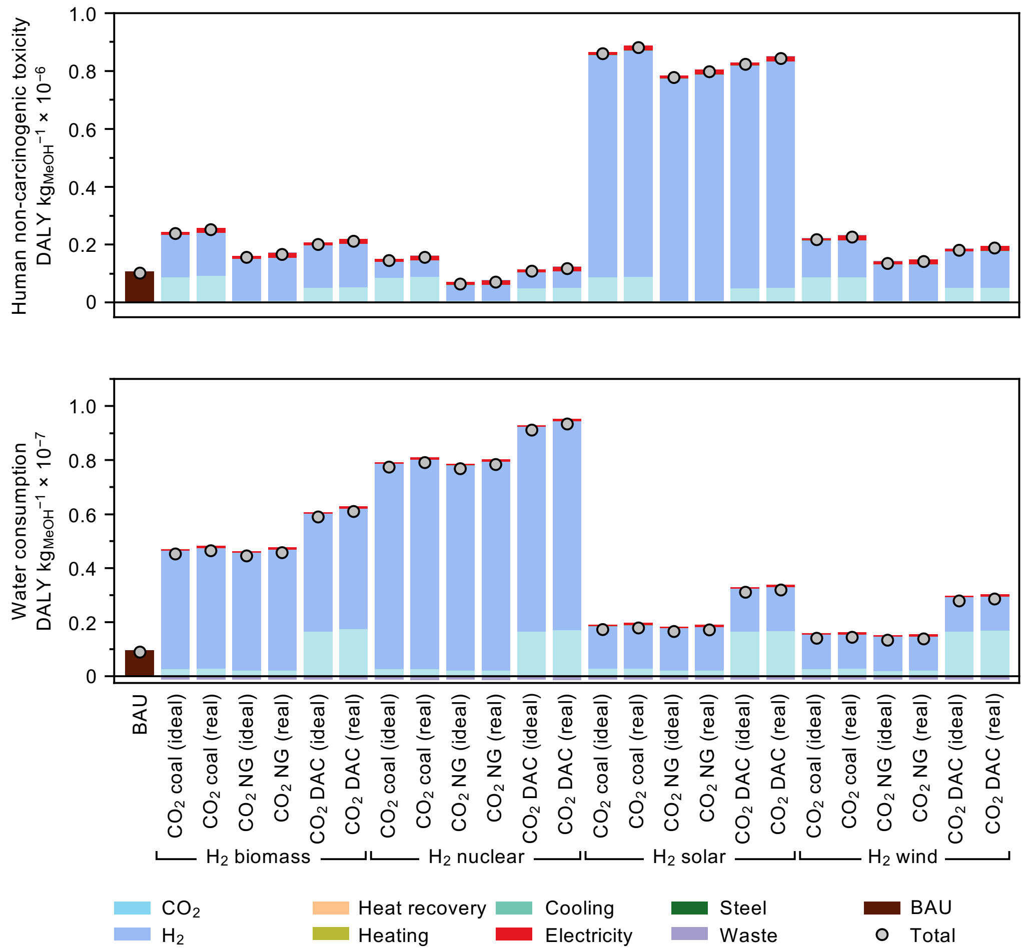

Figure S2a continued. ReCiPe 2016 LCI analysis at the midpoint level of all methanol process scenarios analysed, contributions to human health.

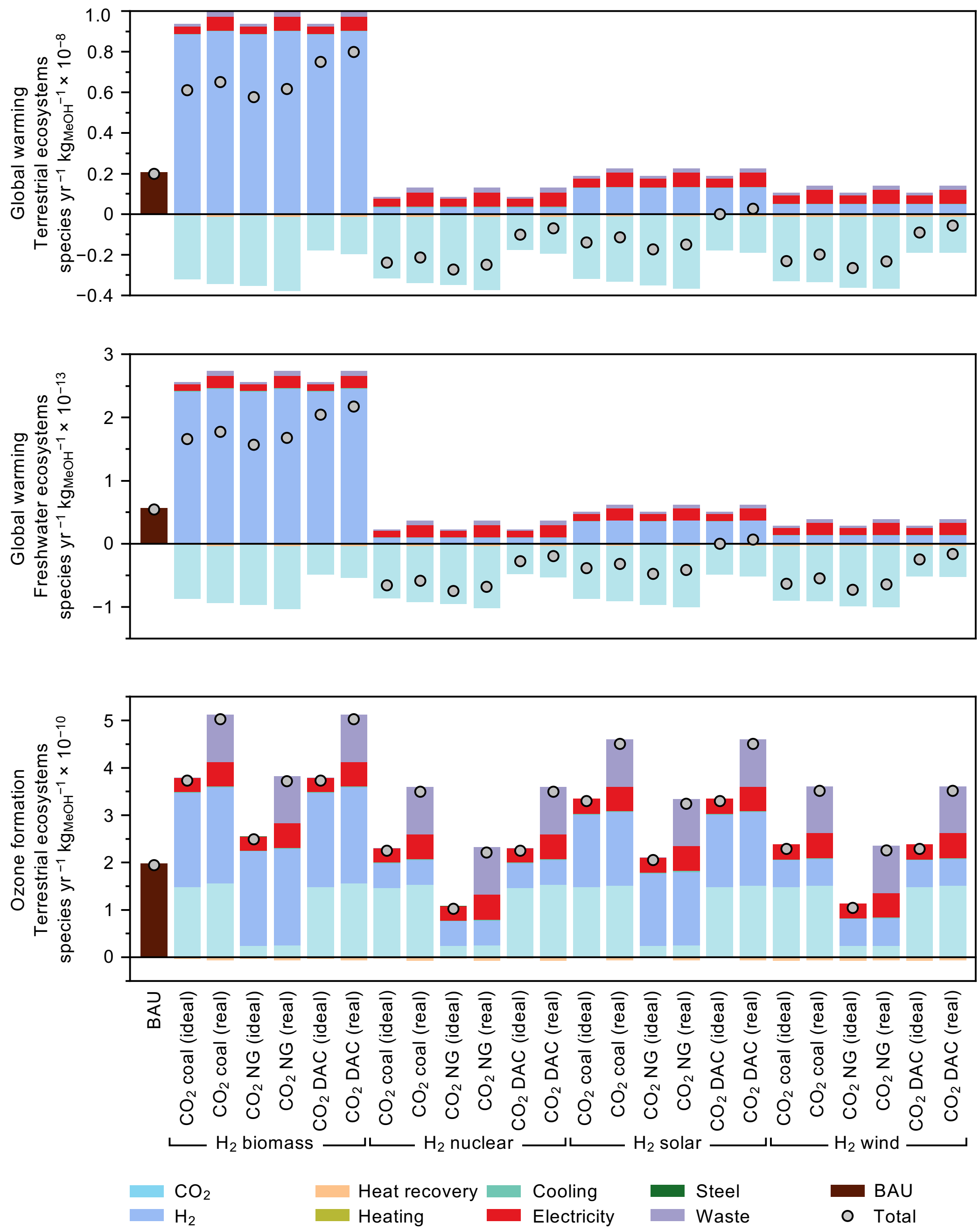

Figure S2b. ReCiPe 2016 LCI analysis at the midpoint level of all methanol process scenarios analysed, contributions to ecosystems quality.

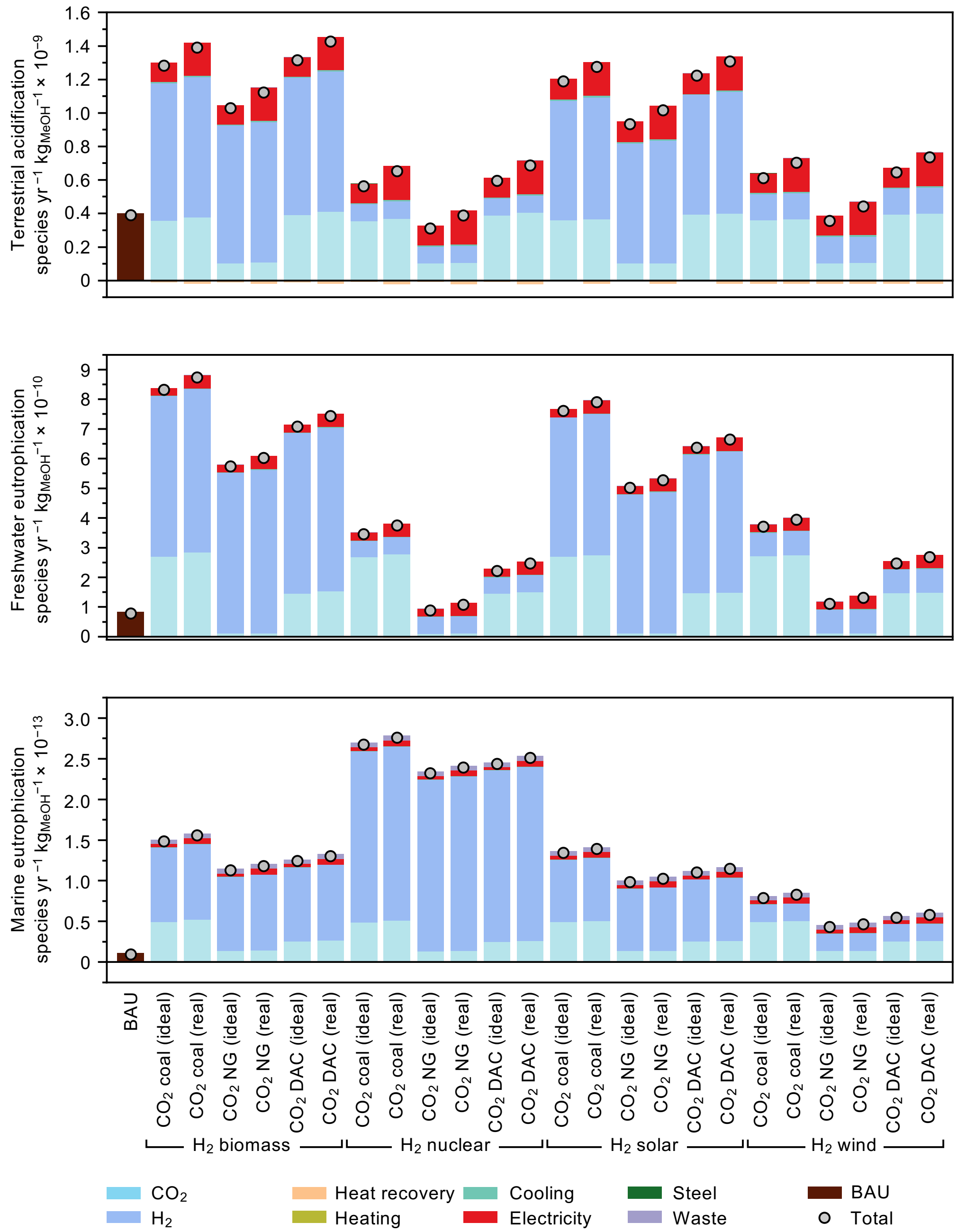

Figure S2b continued. ReCiPe 2016 LCI analysis at the midpoint level of all methanol process scenarios analysed, contributions to ecosystems quality.

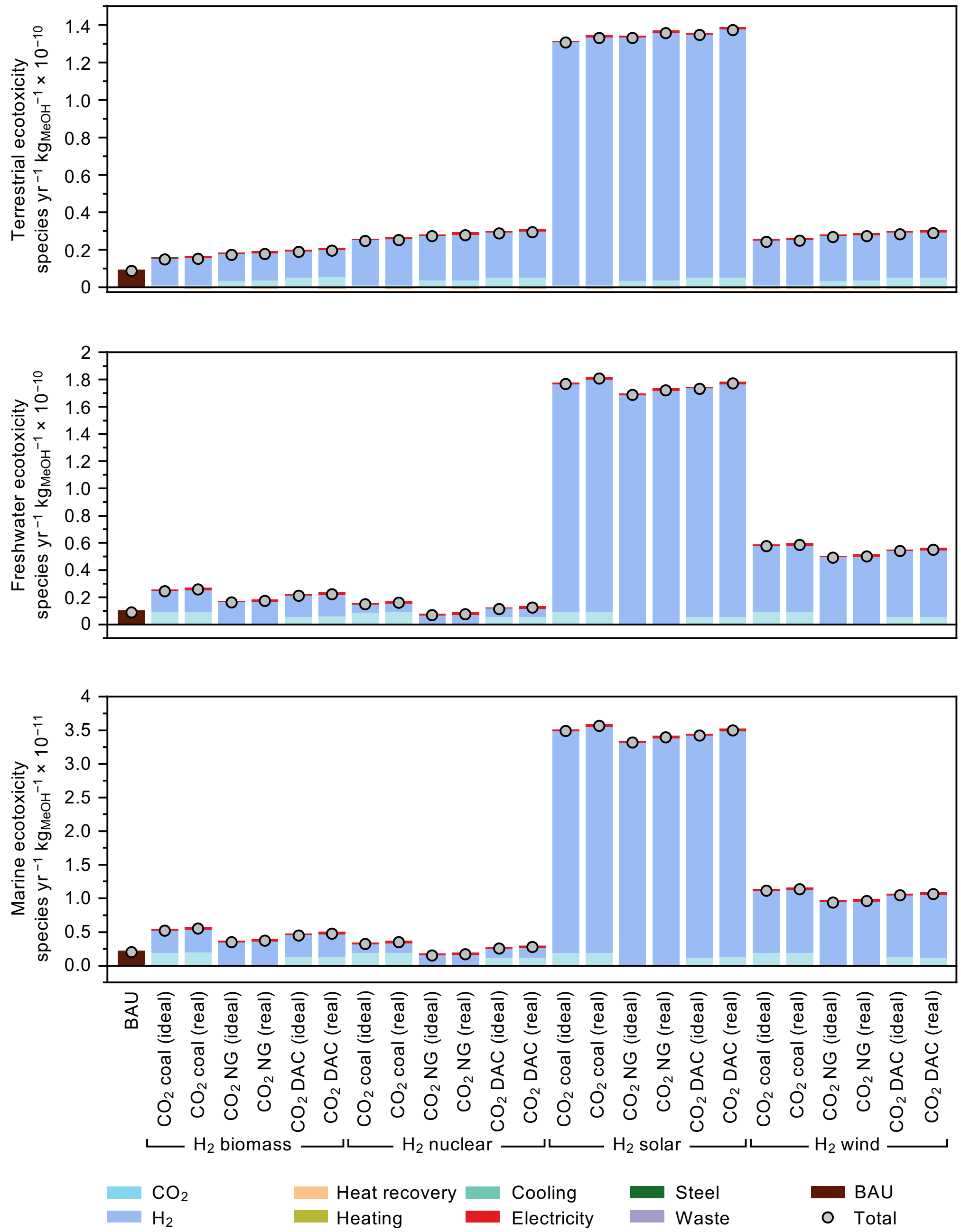

Figure S2b continued. ReCiPe 2016 LCI analysis at the midpoint level of all methanol process scenarios analysed, contributions to ecosystems quality.

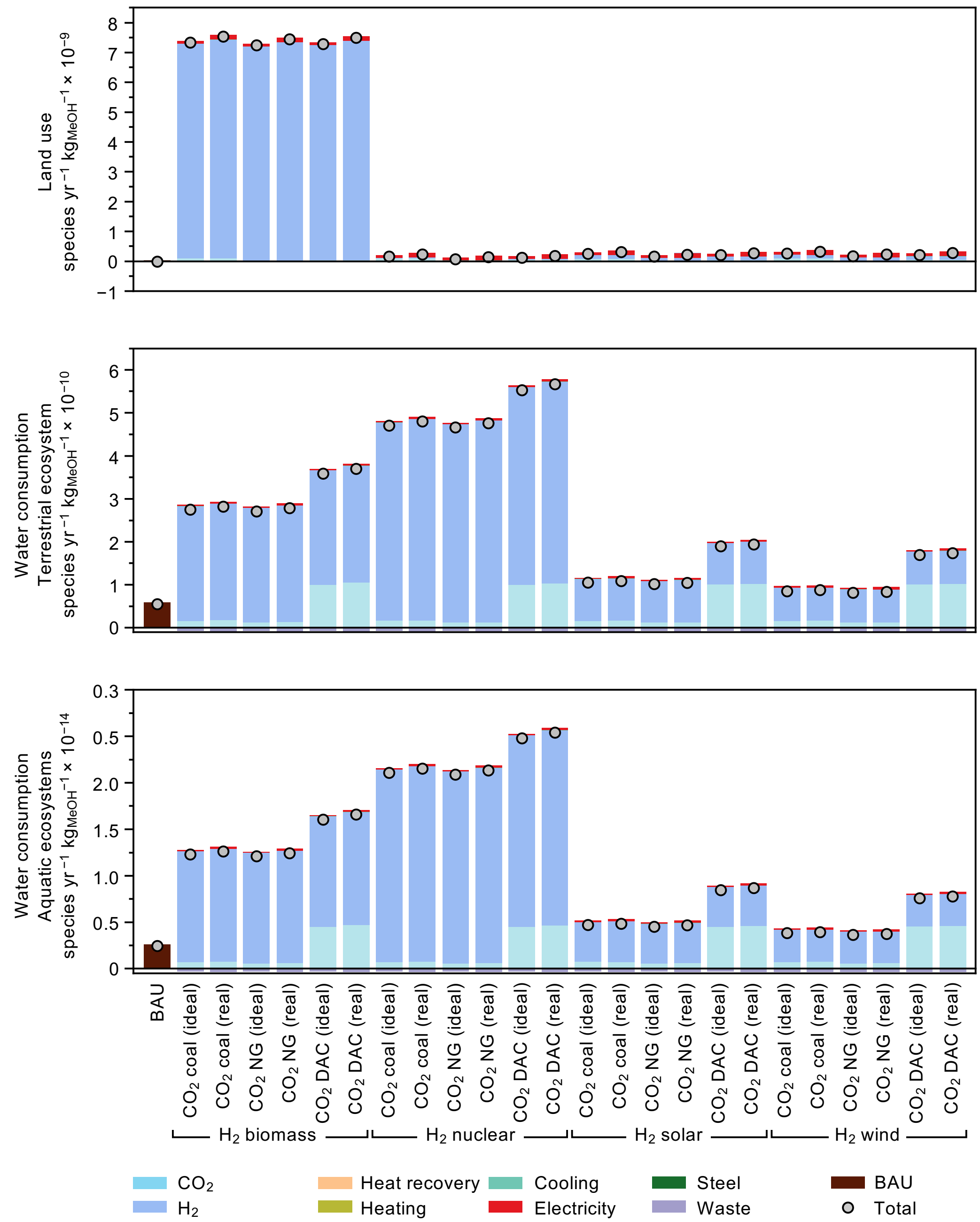

Figure S2b continued. ReCiPe 2016 LCI analysis at the midpoint level of all methanol process scenarios analysed, contributions to ecosystems quality.

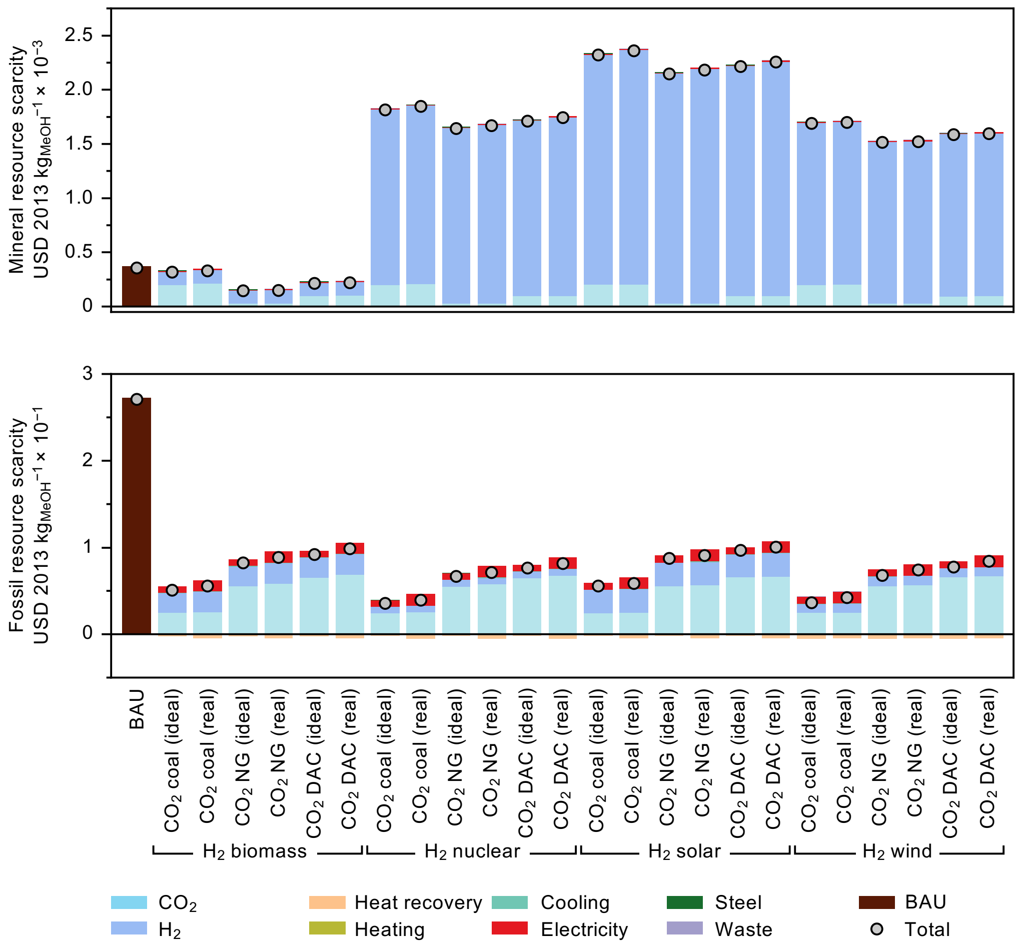

Figure S2c. ReCiPe 2016 LCI analysis at the midpoint level of all methanol process scenarios analysed, contributions to resource scarcity.

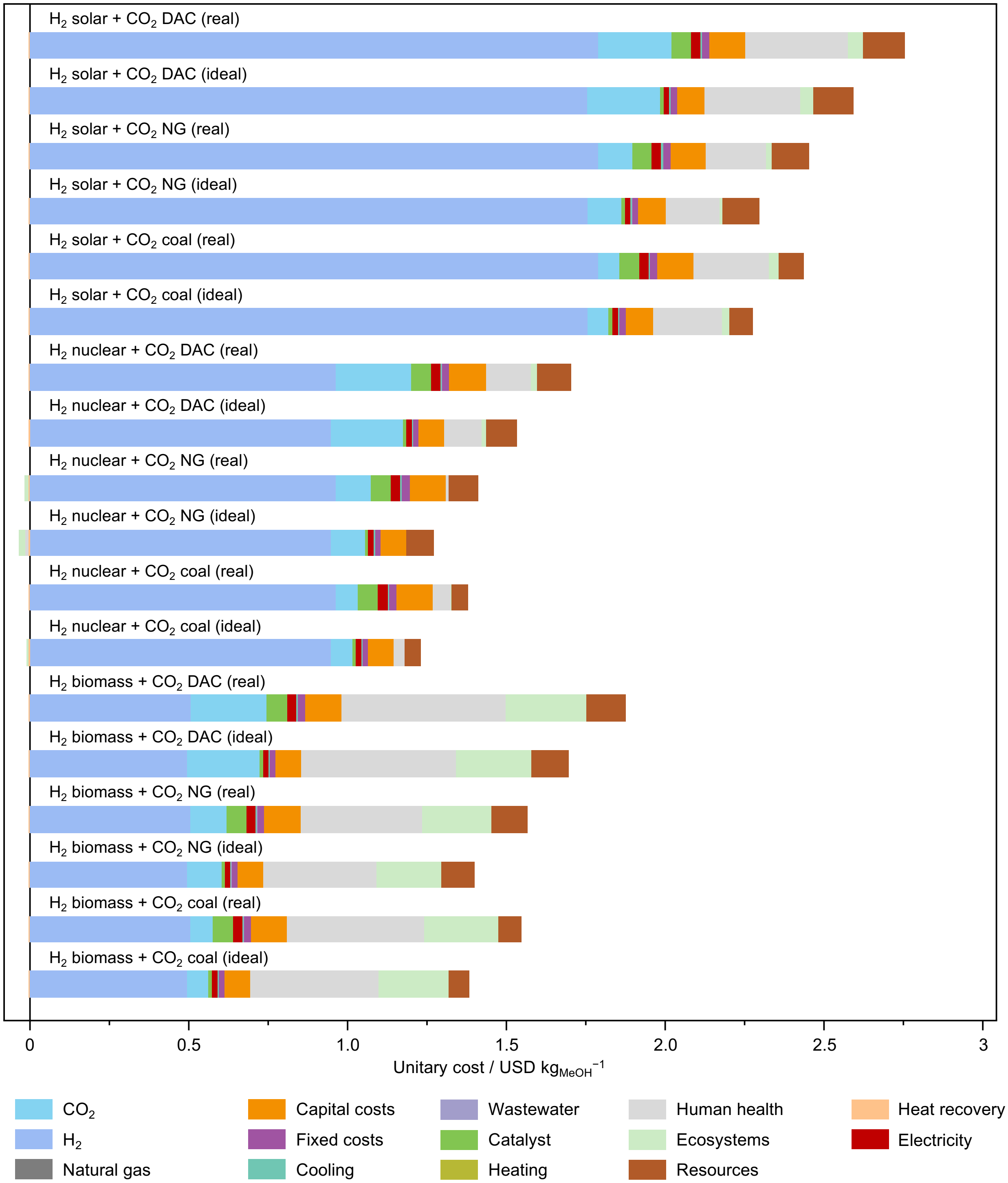

Figure S3. Total cost, including externalities, of methanol from all of the process scenarios analysed. Complementary data to **Figure 3** in the main manuscript.

5. Future costs of hydrogen from water electrolysis

Future hydrogen costs were estimated from prospects on the technical specifications of electrolysis technologies, *i.e.*, CAPEX expenditures, efficiency and useful time, together with estimates of future electricity prices taken from the US Energy Information Administration.[25] The capital cost of the electrolysers, efficiency and stack lifetime reported in **Tables S7-S9** were retrieved from Schmidt *et al.*[26] The CAPEX expenditures were annualised applying the annual capital charge factor proposed by Sinnot and Towler,[6] considering an interest rate of 15%, and a useful time computed from the stack lifetime of the electrolyser available in Schmidt *et al.*[26] The OPEX expenditures were approximated from the amount of electricity consumed per kg of hydrogen generated and the corresponding electricity cost (**Table S1**). The electricity consumption per kg of hydrogen was obtained from the electrolyser efficiency and heat content of hydrogen. Lower and upper bounds on the methanol cost from water electrolysis are provided, which correspond to the best and worst future scenarios. The former assumes the lowest values for the CAPEX of the electrolyser and the electricity costs, and the maximum values for the electrolyser efficiency and useful life time, while the upper bound assumes the highest CAPEX and electricity costs and the lowest efficiencies and useful life times.

As the basis for the calculations, we assumed an enthalpy for water electrolysis of 65.83 kWh $\text{kmol}_{H_2O}^{-1}$, corresponding to 32.92 kWh $\text{kg}_{H_2}^{-1}$. The real energy of water electrolysis referred to 1 kg of H_2 was calculated adjusting this value by the electrolyser efficiency:

$$\text{Real energy} = \frac{\text{Enthalpy of water electrolysis}}{\text{Electrolyser efficiency}} \quad \left[\frac{\text{kWh}}{\text{kg}_{\text{H}_2}}\right]$$

The total amount of H_2 produced per year was calculated assuming 4,500 operating hours, which result in 4,500 kWh per year, given the intermittency of the operation in the electrolyser:

$$\text{Hydrogen production} = \frac{\text{Annual electricity consumption}}{\text{Real energy}} \quad \left[\frac{\text{kg}_{\text{H}_2}}{\text{yr}}\right]$$

The operating costs per kg of H_2 were then calculated as follows:

$$\text{OPEX} = \frac{\text{Annual electricity consumption} \times \text{Electricity cost in 2030}}{\text{Hydrogen production}} \quad \left[\frac{\text{EUR}}{\text{kg}_{\text{H}_2}}\right]$$

The CAPEX per kg of H_2 were calculated by multiplying the total capital cost of the electrolyser by its corresponding annual capital charge (ACC):

$$\text{CAPEX} = \frac{\text{Electrolyser capital cost} \times \text{ACC}}{\text{Hydrogen production}} \quad \left[\frac{\text{EUR}}{\text{kg}_{\text{H}_2}}\right]$$

Externalities for H_2 were calculated following the approach reported in Section 2.

The total cost was finally calculated as the sum of OPEX, CAPEX and H_2 externalities in the corresponding cases. The calculations were performed using EUR and converting the final results into USD using a factor of 1.1. The methanol costs for the various projected costs of H_2 are compiled in **Table S10**.

Table S7. Hydrogen cost projections for water electrolysis powered by wind electrolysis.

	Wind electricity + externalities						Wind electricity					
Electrolyser	AEC		PEMEC		SOEC		AEC		PEMEC		SOEC	
Bound	min	max	min	max	min	max	min	max	min	max	min	max
Electrolysis												
Enthalpy of water electrolysis referred to H_2 (kWh $kg_{H_2}^{-1}$)	32.9	32.9	32.9	32.9	32.9	32.9	32.9	32.9	32.9	32.9	32.9	32.9
Real energy of water electrolysis referred to H_2 (kWh $kg_{H_2}^{-1}$)	47.7	52.2	42.2	52.2	40.1	40.1	47.7	52.2	42.2	52.2	40.1	40.1
H_2 production (kg yr^{-1})	94.3	86.1	106.6	86.1	112.1	112.1	94.3	86.1	106.6	86.1	112.1	112.1
Operating costs												
Electricity cost (EUR kWh^{-1}) 2030	0.034	0.055	0.034	0.055	0.034	0.055	0.034	0.055	0.034	0.055	0.034	0.055
OPEX future (EUR $kg_{H_2}^{-1}$)	1.623	2.883	1.436	2.883	1.366	2.215	1.623	2.883	1.436	2.883	1.366	2.215
Capital costs												
Capital cost (EUR kW^{-1})	350	550	400	1320	550	2500	350	550	400	1320	550	2500
Electrolyser efficiency (%LHV based)	0.69	0.63	0.78	0.63	0.82	0.82	0.69	0.63	0.78	0.63	0.82	0.82
Stack lifetime (h)	82500	82500	90000	80000	115000	35000	82500	82500	90000	80000	115000	35000
Electricity consumption (kWh yr^{-1})	4500	4500	4500	4500	4500	4500	4500	4500	4500	4500	4500	4500
Stack lifetime (yr)	18	18	20	18	26	8	18	18	20	18	26	8
Annual capital charge (ACC)	0.163	0.163	0.160	0.164	0.154	0.226	0.163	0.163	0.160	0.164	0.154	0.226
Annualised capital cost (EUR kW^{-1} yr^{-1})	56.89	89.39	63.90	216.00	84.89	565.79	56.89	89.39	63.90	216.00	84.89	565.79
Capital cost per kg H_2 (EUR kg^{-1})	0.603	1.038	0.599	2.508	0.757	5.047	0.603	1.038	0.599	2.508	0.757	5.047
Externalities												
Externalities (EUR $kg_{H_2}^{-1}$)	0.102	0.102	0.102	0.102	0.102	0.102	n.a.	n.a.	n.a.	n.a.	n.a.	n.a.
Total												
Projected cost of H_2 2030 (EUR $kg_{H_2}^{-1}$)	2.328	4.022	2.137	5.492	2.224	7.363	2.226	3.921	2.035	5.391	2.123	7.262
Projected cost of H_2 2030 (USD $kg_{H_2}^{-1}$)	2.560	4.424	2.350	6.041	2.447	8.100	2.449	4.313	2.238	5.930	2.335	7.988

Table S8. Hydrogen cost projections for water electrolysis powered by nuclear electrolysis.

	Nuclear electricity + externalities						Nuclear electricity					
Electrolyser	AEC		PEMEC		SOEC		AEC		PEMEC		SOEC	
Bound	min	max	min	max	min	max	min	max	min	max	min	max
Electrolysis												
Enthalpy of water electrolysis referred to H_2 (kWh $kg_{H_2}^{-1}$)	32.9	32.9	32.9	32.9	32.9	32.9	32.9	32.9	32.9	32.9	32.9	32.9
Real energy of water electrolysis referred to H_2 (kWh $kg_{H_2}^{-1}$)	47.7	52.2	42.2	52.2	40.1	40.1	47.7	52.2	42.2	52.2	40.1	40.1
H_2 production (kg yr^{-1})	94.3	86.1	106.6	86.1	112.1	112.1	94.3	86.1	106.6	86.1	112.1	112.1
Operating costs												
Electricity cost (EUR kWh^{-1}) 2030	0.037	0.051	0.037	0.051	0.037	0.051	0.037	0.051	0.037	0.051	0.037	0.051
OPEX future (EUR $kg_{H_2}^{-1}$)	1.782	2.666	1.576	2.666	1.499	2.048	1.782	2.666	1.576	2.666	1.499	2.048
Capital costs												
Capital cost (EUR kW^{-1})	350	550	400	1320	550	2500	350	550	400	1320	550	2500
Electrolyser efficiency (%LHV based)	0.69	0.63	0.78	0.63	0.82	0.82	0.69	0.63	0.78	0.63	0.82	0.82
Stack lifetime (h)	82500	82500	90000	80000	115000	35000	82500	82500	90000	80000	115000	35000
Electricity consumption (kWh yr^{-1})	4500	4500	4500	4500	4500	4500	4500	4500	4500	4500	4500	4500
Stack lifetime (yr)	18	18	20	18	26	8	18	18	20	18	26	8
Annual capital charge (ACC)	0.163	0.163	0.160	0.164	0.154	0.226	0.163	0.163	0.160	0.164	0.154	0.226
Annualised capital cost (EUR kW^{-1} yr^{-1})	56.89	89.39	63.90	216.00	84.89	565.79	56.89	89.39	63.90	216.00	84.89	565.79
Capital cost per kg H_2 (EUR kg^{-1})	0.603	1.038	0.599	2.508	0.757	5.047	0.603	1.038	0.599	2.508	0.757	5.047
Externalities												
Externalities (EUR $kg_{H_2}^{-1}$)	0.085	0.085	0.085	0.085	0.085	0.085	n.a.	n.a.	n.a.	n.a.	n.a.	n.a.
Total												
Projected cost of H_2 2030 (EUR $kg_{H_2}^{-1}$)	2.470	3.789	2.261	5.259	2.342	7.181	2.385	3.704	2.175	5.174	2.257	7.096
Projected cost of H_2 2030 (USD $kg_{H_2}^{-1}$)	2.717	4.168	2.487	5.785	2.576	7.899	2.623	4.075	2.393	5.692	2.482	7.805

Table S9. Hydrogen cost projections for water electrolysis powered by solar electrolysis.

	Solar electricity + externalities						Solar electricity					
Electrolyser	AEC		PEMEC		SOEC		AEC		PEMEC		SOEC	
Bound	min	max	min	max	min	max	min	max	min	max	min	max
Electrolysis												
Enthalpy of water electrolysis referred to H_2 (kWh $kg_{H_2}^{-1}$)	32.9	32.9	32.9	32.9	32.9	32.9	32.9	32.9	32.9	32.9	32.9	32.9
Real energy of water electrolysis referred to H_2 (kWh $kg_{H_2}^{-1}$)	47.7	52.2	42.2	52.2	40.1	40.1	47.7	52.2	42.2	52.2	40.1	40.1
H_2 production (kg yr^{-1})	94.3	86.1	106.6	86.1	112.1	112.1	94.3	86.1	106.6	86.1	112.1	112.1
Operating costs												
Electricity cost (EUR kWh^{-1}) 2030	0.035	0.053	0.035	0.053	0.035	0.053	0.035	0.053	0.035	0.053	0.035	0.053
OPEX future (EUR $kg_{H_2}^{-1}$)	1.649	2.751	1.458	2.751	1.387	2.113	1.649	2.751	1.458	2.751	1.387	2.113
Capital costs												
Capital cost (EUR kW^{-1})	350	550	400	1320	550	2500	350	550	400	1320	550	2500
Electrolyser efficiency (%LHV based)	0.69	0.63	0.78	0.63	0.82	0.82	0.69	0.63	0.78	0.63	0.82	0.82
Stack lifetime (h)	82500	82500	90000	80000	115000	35000	82500	82500	90000	80000	115000	35000
Electricity consumption (kWh yr^{-1})	4500	4500	4500	4500	4500	4500	4500	4500	4500	4500	4500	4500
Stack lifetime (yr)	18	18	20	18	26	8	18	18	20	18	26	8
Annual capital charge (ACC)	0.163	0.163	0.160	0.164	0.154	0.226	0.163	0.163	0.160	0.164	0.154	0.226
Annualised capital cost (EUR kW^{-1} yr^{-1})	56.89	89.39	63.90	216.00	84.89	565.79	56.89	89.39	63.90	216.00	84.89	565.79
Capital cost per kg H_2 (EUR kg^{-1})	0.603	1.038	0.599	2.508	0.757	5.047	0.603	1.038	0.599	2.508	0.757	5.047
Externalities												
Externalities (EUR $kg_{H_2}^{-1}$)	0.303	0.303	0.303	0.303	0.303	0.303	n.a.	n.a.	n.a.	n.a.	n.a.	n.a.
Total												
Projected cost of H_2 2030 (EUR $kg_{H_2}^{-1}$)	2.555	4.092	2.361	5.562	2.447	7.463	2.252	3.789	2.058	5.259	2.145	7.161
Projected cost of H_2 2030 (USD $kg_{H_2}^{-1}$)	2.810	4.501	2.597	6.118	2.692	8.210	2.477	4.168	2.264	5.785	2.359	7.877

Table S10. Projected methanol prices in 2030.

Electrolyser	AEC		PEMEC		SOEC	
Bound	min	max	min	max	min	max
CO_2 coal + H_2 wind	0.785	1.154	0.743	1.473	0.762	1.881
CO_2 coal + H_2 nuclear	0.812	1.095	0.768	1.409	0.785	1.819
CO_2 coal + H_2 solar	0.789	1.124	0.747	1.444	0.766	1.857
CO_2 NG + H_2 wind	0.826	1.194	0.784	1.514	0.803	1.921
CO_2 NG + H_2 nuclear	0.854	1.136	0.809	1.450	0.826	1.861
CO_2 NG + H_2 solar	0.830	1.164	0.788	1.484	0.807	1.898
CO_2 DAC + H_2 wind	0.949	1.318	0.908	1.638	0.927	2.045
CO_2 DAC + H_2 nuclear	0.979	1.261	0.934	1.575	0.951	1.986
CO_2 DAC + H_2 solar	0.953	1.288	0.911	1.608	0.930	2.021
CO_2 coal + H_2 wind + externalities	0.913	1.282	0.872	1.602	0.891	2.009
CO_2 coal + H_2 nuclear + externalities	0.924	1.206	0.879	1.520	0.896	1.931
CO_2 coal + H_2 solar + externalities	1.135	1.470	1.093	1.790	1.112	2.203
CO_2 NG + H_2 wind + externalities	0.932	1.300	0.890	1.620	0.909	2.027
CO_2 NG + H_2 nuclear + externalities	0.942	1.224	0.898	1.539	0.915	1.949
CO_2 NG + H_2 solar + externalities	1.154	1.488	1.112	1.808	1.130	2.222
CO_2 DAC + H_2 wind + externalities	1.233	1.601	1.191	1.921	1.210	2.328
CO_2 DAC + H_2 nuclear + externalities	1.247	1.529	1.202	1.843	1.219	2.254
CO_2 DAC + H_2 solar + externalities	1.454	1.789	1.412	2.108	1.431	2.522

6. PBs results and limitations

Figures S4 depicts the impact of methanol production using CO_2 captured from coal or NG plants and through DAC and renewable hydrogen from various sources over the commercial Cu-ZnO-Al_2O_3 catalyst on the PBs.

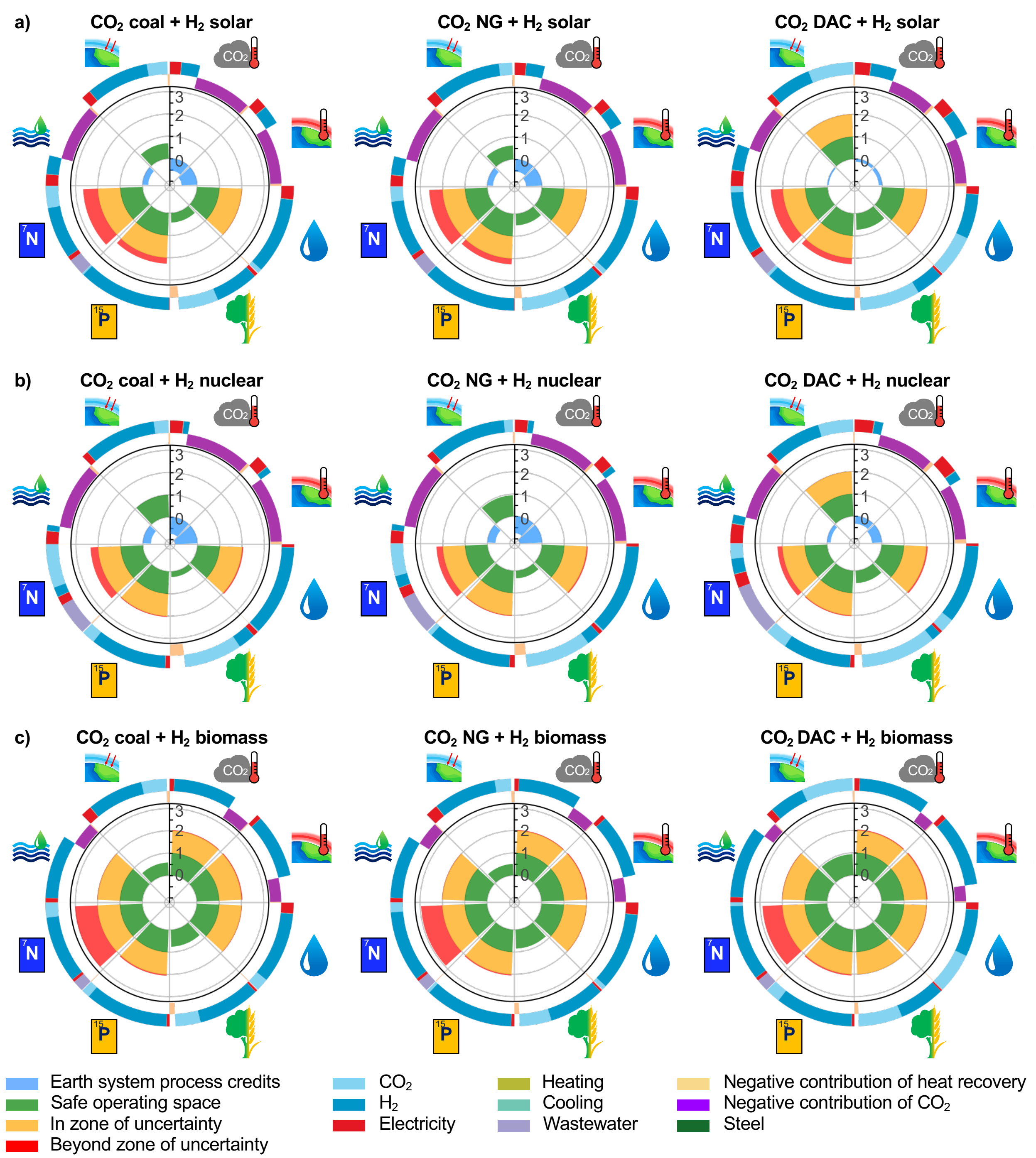

Figure S4. Planet-level performance of methanol production using CO_2 captured from coal or NG plants and renewable hydrogen from **a)** solar, **b)** nuclear or **c)** biomass over the commercial Cu-ZnO-Al_2O_3 catalyst. PBs symbols are defined in **Figure 5** of the main manuscript.

As indicated for the LCA, we also want to stress that the PBs method shows some limitations. These are mainly related to the uncertainties involved in the quantification of global ecological limits[27] and the performance of technologies in terms of these limits.[28] These uncertainties stem from: (i) imprecise global ecological limits yet considered as rough estimates; (ii) the allocation method of choice to assign shares of the safe operating space; (iii) imprecise measurements of the elementary flows needed to compute the PBs, *e.g.*, CO_2 emissions to air; and (iv) uncertainties in the impact model that converts these flows into PBs, *e.g.*, impact on energy imbalance per unit of CO_2 emitted. Future work should, therefore, focus on reducing these uncertainties by defining more accurate ecological limits and fair and robust sharing principles, improving data collection on emissions and developing more accurate damage models to translate emissions into PBs. The definition of fair sharing principles collectively ensuring sustainable development will also require social and political efforts.

We want to highlight that we focused here only on those PBs for which characterisation factors are available. Hence, as an example, biosphere integrity, regarded as a core planetary boundary,[29] was omitted due to the lack of robust methods to carry out the calculations.

References

1 W. L. Luyben, *Ind. Eng. Chem. Res.*, 2010, **49**, 6150–6163.
2 K. M. Vanden Bussche and G. F. Froment, *J. Catal.*, 1996, **161**, 1–10.
3 M. Pérez-Fortes, J. C. Schöneberger, A. Boulamanti and E. Tzimas, *Appl. Energy*, 2016, **161**, 718–732.
4 A. Gonzalez-Garay and G. Guillen-Gosalbez, *Chem. Eng. Res. Des.*, 2018, **137**, 1711–1716.
5 T. F. Yee, I. E. Grossmann and Z. Kravanja, *Comput. Chem. Eng.*, 1990, **14**, 1151–1164.
6 G. Towler and R. Sinnott, *Chemical Engineering Design. Principles, practice and economics of plant and process design*, 2008.
7 E. S. Rubin, J. E. Davison and H. J. Herzog, *Int. J. Greenh. Gas Control*, 2015, **40**, 378–400.
8 D. W. Keith, G. Holmes, D. St. Angelo and K. Heidel, *Joule*, 2018, **2**, 1573–1594.
9 B. Parkinson, P. Balcombe, J. F. Speirs, A. D. Hawkes and K. Hellgardt, *Energy Environ. Sci*, 2019, **12**, 19.
10 W. D. Seider, J. D. Seader, D. R. Lewin and S. Widagdo, *Product and process design principles : synthesis, analysis, and evaluation*, John Wiley & Sons, US, 3rd ed., 2009.
11 M. Martín and I. E. Grossmann, *AIChE J.*, 2012, **58**, 1538–1549.
12 G. Wernet, C. Bauer, B. Steubing, J. Reinhard, E. Moreno-Ruiz, B. B. Weidema, R. Zah and W. Org, *Int. J. Life Cycle Assess.*, 2016, **21**, 1218–1230.
13 M. A. J. Huijbregts, Z. J. N. Steinmann, P. M. F. Elshout, G. Stam, F. Verones, M. Vieira, M. Zijp, A. Hollander and R. van Zelm, *Int. J. Life Cycle Assess.*, 2017, **22**, 138–147.
14 J. C. Abanades, E. S. Rubin, M. Mazzotti and H. J. Herzog, *Energy Environ. Sci.*, 2017, **10**, 2491–2499.
15 B. P. Weidema, *J. Ind. Ecol.*, 2015, **19**, 20–26.
16 A. Mehmeti, A. Angelis-Dimakis, G. Arampatzis, S. McPhail and S. Ulgiati, *Environments*, 2018, **5**, 24.
17 D. Iribarren, F. Petrakopoulou and J. Dufour, *Energy*, 2013, **50**, 477–485.
18 F. Petrakopoulou, D. Iribarren and J. Dufour, *Greenh. Gases Sci. Technol.*, 2015, **5**, 268–276.
19 R. M. Cuéllar-Franca and A. Azapagic, *J. CO2 Util.*, 2015, **9**, 82–102.
20 A. Susmozas, D. Iribarren and J. Dufour, *Resources*, 2015, **4**, 398–411.
21 V. Utgikar and T. Thiesen, *Int. J. Hydrogen Energy*, 2006, **31**, 939–944.
22 E. Cetinkaya, I. Dincer and G. F. Naterer, *Int. J. Hydrogen Energy*, 2012, **37**, 2071–2080.
23 P. L. Spath and M. K. Mann, *Life Cycle Assessment of Renewable Hydrogen Production via Wind/Electrolysis Milestone Completion Report*, 2004.
24 A. Susmozas, D. Iribarren and J. Dufour, *Resources*, 2015, **4**, 398–411.
25 *Us Eia Lcoe*, 2019, 1–25.
26 O. Schmidt, A. Gambhir, I. Staffell, A. Hawkes, J. Nelson and S. Few, *Int. J. Hydrogen Energy*, 2017, **42**, 30470–30492.
27 J. Rockström, W. Steffen, K. Noone, Å. Persson, F. S. Chapin, E. F. Lambin, T. M. Lenton, M. Scheffer, C. Folke, H. J. Schellnhuber, B. Nykvist, C. A. de Wit, T. Hughes, S. van der Leeuw, H. Rodhe, S. Sörlin, P. K. Snyder, R. Costanza, U. Svedin, M. Falkenmark, L. Karlberg, R. W. Corell, V. J. Fabry, J. Hansen, B. Walker, D. Liverman, K. Richardson, P. Crutzen and J. A. Foley, *Nature*, 2009, **461**, 472–475.
28 M. W. Ryberg, M. Owsianiak, K. Richardson and M. Z. Hauschild, *Ecol. Indic.*, 2018, **88**, 250–262.
29 W. Steffen, K. Richardson, J. Rockström, S. E. Cornell, I. Fetzer, E. M. Bennett, R. Biggs, S. R. Carpenter, W. de Vries, C. A. de Wit, C. Folke, D. Gerten, J. Heinke, G. M. Mace, L. M. Persson, V. Ramanathan, B. Reyers and S. Sorlin, *Science (80-.)*, 2015, **347**, 1–11.